Experimental investigation of nonequilibrium capillarity effects: Fluid viscosity effects

Gaurav Goel[1] and Denis M. O'Carroll[2,3]

Received 9 August 2010; revised 23 May 2011; accepted 19 July 2011; published 7 September 2011.

[1] Numerical models have been widely used to simulate multiphase flow in porous media for a variety of applications (e.g., NAPL migration in subsurface aquifers, carbon sequestration, agriculture, paper production, and petroleum reservoir development). The relationship between the difference in phase pressures and saturation is used as one of the important constitutive relationships in numerical models. Theoretical studies have suggested that this relationship should include a damping coefficient or capillarity coefficient (τ) on the basis of thermodynamic considerations. A literature review suggests that the magnitude of this capillarity coefficient varies by over three orders of magnitude. While recent experimental studies have explored the effect of porous medium properties, effect of domain size, hysteresis, and the imposed boundary conditions on the magnitude of τ, there has been no experimental study investigating the impact of fluid viscosity on τ. This study reports on a series of primary drainage experiments conducted under both static and dynamic conditions in F70 silica sand. Fluid pairs used included water and silicone oil with two differing viscosities and slightly different densities (used as model nonaqueous phase liquids) in addition to air. Water saturation and both wetting and nonwetting phase pressures were measured in a custom-built aluminum column using EC-5 probes and tensiometers at three levels. Results show a strong dependence of the magnitude of the capillarity coefficient on effective fluid viscosity. This implies that consideration should be given for the inclusion of a capillarity coefficient in modeling tools used to simulate multiphase flow when fluids saturations are changing rapidly and when fluids have a large viscosity ratio.

Citation: Goel, G., and D. M. O'Carroll (2011), Experimental investigation of nonequilibrium capillarity effects: Fluid viscosity effects, *Water Resour. Res., 47*, W09507, doi:10.1029/2010WR009861.

1. Introduction

[2] The relationship between differences in phase pressure, denoted as ($P_n - P_w$), and saturation is a commonly used constitutive relationship for the simulation of multiphase flow scenarios in the subsurface (e.g., nonaqueous phase liquid [NAPL] contamination, CO_2 sequestration, and agricultural applications). This relationship, $(P_n - P_w) - S_w$, is traditionally assumed to be independent of the rate of saturation change, however, several experimental studies have reported that it is dependent on the rate of change of saturation [e.g., *Topp et al.*, 1967; *Smiles et al.*, 1971; *Stauffer*, 1978; *Kalaydjian*, 1992; *Wildenschild et al.*, 2001; *Hassanizadeh et al.*, 2002; *O'Carroll et al.*, 2005; *Oung et al.*, 2005; *Bottero et al.*, 2006; *Manthey*, 2006; *Camps-Roach et al.*, 2010; *Sakaki et al.*, 2010]. These studies suggest that use of a constitutive relationship that does not account for this rate dependence when simulating scenarios when fluid saturations change rapidly may result in poor simulation predictions.

[3] The underlying phenomenon responsible for this rate dependence is an area of active discussion in the literature and a variety of different phenomena responsible for observed effects have been postulated. For example, a variety of groups have suggested that physical processes (e.g., air and water entrapment, pore water blockage, air entry value effect, and dynamic contact angle) are responsible for this rate dependence [*Friedman*, 1999; *Wildenschild et al.*, 2001]. *Hassanizadeh et al.* [2002] challenged the arguments related to water entrapment, pore water blockage, air entrapment, and dynamic contact angle. One recent core scale air/water experimental study, conducted using two sands, supports these observations with the minor caveat that dynamic contact angle alone does not account for observed effects but could be a contributing factor [*Camps-Roach et al.*, 2010]. Another recent study suggests that the magnitude of this rate dependence is a function of fluid/fluid/solid contact line friction in addition to fluid viscosities [*O'Carroll et al.*, 2010]. Contact line friction is a function of the equilibrium contact angle, interfacial tension, and other fluid properties. These effects have also been attributed to pore scale processes, such as Haines jumps and the finite redistribution time required for fluids to minimize free energy in a pore space following a perturbation

[1]Department of Civil Engineering, Sharda University, Greater Noida, India.
[2]Department of Civil and Environmental Engineering, University of Western Ontario, London, Ontario, Canada.
[3]Also at School of Civil and Environmental Engineering, University of New South Wales, Manly Vale, New South Wales, Australia.

0043-1397/11/2010WR009861

[*Barenblatt*, 1971; *Kalaydjian*, 1992; *Barenblatt et al.*, 2003; *O'Carroll et al.*, 2005]. These processes are not included in larger scale, continuum-based conceptual models. Recent studies have used dynamic pore network models to incorporate pore scale processes [*Dahle et al.*, 2005; *Joekar-Niasar et al.*, 2010; *Joekar-Niasar and Hassanizadeh*, 2011]. These studies found that fluid viscosity plays an important role in the magnitude of observed effects as will be discussed in detail later. It has also been suggested that the presence of microscale heterogeneities/lenses could be responsible for the rate dependence in $(P_n - P_w) - S_w$ [*Hassanizadeh et al.*, 2002; *Manthey et al.*, 2005; *Mirzaei and Das*, 2007]. Other modeling studies suggest that the rate dependence in $(P_n - P_w) - S_w$ results from the averaging of pressures and saturations, and thus domain size [*Dahle et al.*, 2005; *Manthey et al.*, 2005], however, a recent experimental study suggests that observed effects are independent of domain size [*Camps-Roach et al.*, 2010]. Although a number of studies have investigated the underlying mechanisms leading to the rate dependence, significant questions remain. While experimental studies have explored the effect of porous medium properties, domain size, hysteresis, and imposed boundary conditions [e.g., *Bottero*, 2009; *Camps-Roach et al.*, 2010; *Sakaki et al.*, 2010] no experimental study has investigated the effect of fluid viscosity on the rate dependence of $(P_n - P_w) - S_w$.

[4] A variety of mathematical relationships have been proposed to relate fluid phase pressures to fluid saturation when saturations are changing [e.g., *Barenblatt*, 1971; *Stauffer*, 1978; *Hassanizadeh and Gray*, 1990; *Kalaydjian*, 1992; *Silin and Patzek*, 2004]. Barenblatt and coworkers proposed that a finite redistribution time is required for fluid rearrangement, and therefore free-energy minimization, in a pore space following a perturbation [*Barenblatt*, 1971; *Barenblatt et al.*, 2003; *Silin and Patzek*, 2004]. Their conceptual model uses fluid saturation at a future time to determine differences in phase pressure at the current time when fluid saturations are changing. The model of *Hassanizadeh and Gray* [1990, 1991b, 1991a, 1993b, 1993a] and that of *Kalaydjian* [1992] are based on thermodynamic considerations with the difference in fluid phase pressures under dynamic and equilibrium conditions a linear function of the rate of saturation change:

$$(P_n - P_w) - P_c^s = -\tau \frac{\partial S_w}{\partial t}, \tag{1}$$

where P_n is nonwetting phase pressure, P_w is wetting phase pressure, P_c^s is the difference in phase pressures measured under static or equilibrium conditions, $\frac{\partial S_w}{\partial t}$ is the rate of change of wetting phase saturation, and τ is a capillarity or dynamic coefficient. On the basis of a detailed literature review, τ was estimated to be in the range of 3×10^4 to 10^7 kg/m^{-1}/s^{-1} [*Hassanizadeh et al.*, 2002], which is consistent with values derived from more recent PCE (tetrachloroethene)-water and air-water experiments [*O'Carroll et al.*, 2005; *Oung et al.*, 2005; *Bottero et al.*, 2006; *Bottero*, 2009; *Camps-Roach et al.*, 2010; *Sakaki et al.*, 2010]. The large range of reported τ suggests that further work is required to develop a deeper understanding of the reasons for these variations.

[5] The empirical relationship of *Stauffer* [1978] was developed on the basis of a series of air-water experiments:

$$\tau = \frac{\alpha \phi \mu}{k \lambda} \left(\frac{P_d}{\rho g} \right)^2, \tag{2}$$

where ϕ is porosity, α is a constant with value $= 0.1$, k is intrinsic permeability, μ is water viscosity, ρ is the water density, g is gravity, and P_d and λ are *Brooks-Corey* [1964] model parameters. This equation suggests that τ is a function of both fluid and porous medium properties. Given that equation (2) includes the viscosity of only one fluid in a multiphase flow scenario *Joekar-Niasar and Hassanizadeh* [2011] recommended that the viscosity term be replaced with effective viscosity:

$$\mu_{eff} = \mu_n S_n + \mu_w S_w, \tag{3}$$

where μ_n is the viscosity of the nonwetting phase, S_n is the saturation of the nonwetting phase, μ_w is the viscosity of the wetting phase, and S_w is saturation of the wetting phase.

[6] A number of modeling studies have investigated the impact of fluid viscosity on the rate dependence of $(P_n - P_w) - S_w$ [*Dahle et al.*, 2005; *Manthey*, 2006; *Das et al.*, 2007; *Gielen*, 2007; *Joekar-Niasar et al.*, 2010; *Joekar-Niasar and Hassanizadeh*, 2011]. The studies of *Manthey* [2006] and *Das et al.* [2007] used continuum models where the rate dependence of $(P_n - P_w) - S_w$ was not included in the model governing equations. Their work suggests that the rate dependence can result when fluid phase pressures and saturations, obtained at a fine grid scale, are averaged over a larger domain. In the study of *Das et al.* [2007], τ increased with decreasing viscosity ratio, $\left(\frac{\mu_n}{\mu_w}\right)$, for a portion of the reported saturation range (i.e., $0.2 < S_w < 0.4$); and in the study of *Manthey* [2006] this trend was observed for the entire saturation range. *Das et al.* [2007] suggests that the observed rate dependence, and thus the time for minimization of free energy, is related to the mobility ratio, $\left(\frac{k_{rw}\,\mu_n}{k_{rn}\,\mu_w}\right)$. The studies of *Manthey* [2006] and *Das et al.* [2007] ascribe a different source of the rate dependence (i.e., upscaling of pressures and saturation) than studies that have ascribed physical phenomena to observed effects (e.g., Haines jumps or redistribution time). A recent experimental study observed the rate dependence at the representative elementary volume (REV) scale and found that these effects were similar when fluid phase pressures and saturation were averaged at the column scale suggesting that upscaling was not the source of the observed rate dependence [*Camps-Roach et al.*, 2010]. The studies of *Gielen* [2007], *Joekar-Niasar et al.* [2010], and *Joekar-Niasar and Hassanizadeh* [2011] found the opposite trend (i.e., τ increases with increasing viscosity ratio) than that of *Das et al.* [2007] using a pore network modeling approach. They employed similar volume-averaging techniques as the aforementioned studies [*Manthey*, 2006; *Das et al.*, 2007]. *Joekar-Niasar et al.* [2010] and *Joekar-Niasar and Hassanizadeh* [2011] suggest that larger viscosity ratios increase the time for fluid interface rearrangement following a disturbance and thus lead to larger times for minimization of

free energy [*Barenblatt et al.*, 2003; *Joekar-Niasar et al.*, 2010; *Joekar-Niasar and Hassanizadeh*, 2011]. This review of modeling literature studies suggests that differing approaches yield conflicting results, none of which have been confirmed experimentally.

[7] The goal of this study was to experimentally determine the impact of fluid viscosity and viscosity ratio on the rate dependence of $(P_n - P_w) - S_w$. A series of primary drainage experiments were conducted under near-static and dynamic conditions using air or one of two silicone oils as the nonwetting phase. Water pressure, nonwetting phase pressure, and water saturation were measured at three measurement locations in the same vertical column. This study first quantified the impact of desaturation rate on the relationship between the difference in phase pressures and saturation for three water/nonwetting fluid phase pairs. This work then investigated the impact of fluid viscosities on the capillarity coefficient τ and evaluated different normalization methods.

2. Materials and Methods

2.1. Materials

[8] The porous media used in all experiments was F70 Ottawa sand (Opta Minerals Inc., Brantford, Ontario). The F70 sand had a mean grain size of 0.018 cm and a uniformity index $\left(d_{60}/d_{10}\right)$ of 1.6. Distilled, de-aired, and deionized (DI) water was used as the aqueous phase in all experiments. Silicone oils (polydimethyl-siloxanes, Clearco Products, PA), with viscosities that varied by nearly an order of magnitude, were used as model nonaqueous phase liquids (NAPL) in addition to air (Table 1). Density difference for the selected silicone oils (i.e., 20%) was much smaller than viscosity differences. As such it is assumed that the primary physical property investigated was fluid viscosity.

2.2. Experimental Setup

[9] All experiments were conducted in a custom-built cylindrical aluminum pressure cell (20 cm long and 10 cm inner diameter). Sets of probes, each comprising of a wetting phase tensiometer, a nonwetting phase tensiometer (NWPT), and a moisture probe, were installed at 7, 10, and 13 cm from the top of the column. The wetting phase tensiometer consisted of a ceramic porous cup (length = 2.86 cm, outer diameter = 0.64, 0652 × 03-B1M3, Soil Moisture Corp., Santa Barbara, CA, USA) that was attached to a Swagelok fitting connected to a pressure transducer (FP 2000, Honeywell, Columbus, OH, USA). To create the NWPT, ceramic cups were placed in 1 M solution of hydrochloric acid for 2 hrs, rinsed thoroughly with DI water and then dried at room temperature for ~12 h. The ceramic cups were then placed in a 2% solution of octedecytrichlorosaline (OTS) (Fisher Scientific, Ottawa, Ontario) in toluene and shaken for 20 min [*Lenhard and Parker*, 1987; *Busby et al.*, 1995; *Hopmans et al.*, 1998]. The excess OTS solution was drained and the cups were rinsed with pure toluene. Finally, the OTS treated cups were oven dried for 1.5 hrs at 100°C before being attached to the Swagelok fittings. Prior to each experiment the untreated and treated ceramic cups were submerged in the wetting (i.e., water) or nonwetting fluid (i.e., air or silicone oil), respectively, and left in a vacuum chamber for 5 hrs. This ensured that the pores of the ceramic cups were thoroughly saturated with the wetting fluid at the beginning of each experiment [*Hopmans et al.*, 1998; *Camps-Roach et al.*, 2010]. Pressure transducers were connected to a data logger (Model CR 3000, Campbell Scientific, Logan, Utah) and calibrated with their respective fluid phase prior to each experiment to ensure measurement precision and accuracy.

[10] Wetting phase saturation was measured using EC-5 soil moisture sensors (Decagon Devices, WA, USA). These probes measured the dielectric permittivity of the medium using the capacitance technique [*Czarnomski et al.*, 2005; *Camps-Roach et al.*, 2010; *Sakaki et al.*, 2010]. Recent studies in reference liquids suggest that these sensors are sensitive in the range of electric permittivities used in this study [*Bogena et al.*, 2007; *Rosenbaum et al.*, 2010]. EC-5 probes were oriented vertically in the column thereby minimizing the cross-sectional area of the column occupied by the probe to avoid interference with fluid flow in the column. Independent experiments were conducted to assess the depth over which water saturation is measured. These experiments suggest that the EC-5 probes are most sensitive when the fluid interface is between the top of the upper EC-5 prong and the bottom of the lower EC-5 prong (a distance of 1.5 cm). There is very limited EC-5 response when the fluid interface is between the top prong and 0.5 cm above, or between the bottom prong and 0.5 cm below, and virtually no response when the fluid interface is outside of this zone. Previous studies that have utilized EC-5 probes to measure water saturation were conducted in air-water systems. The dielectric constant (ε) of silicone oil ($\varepsilon \sim 2.4$) [*Clearco*, 2010] is slightly larger than air ($\varepsilon \sim 1$) and considerably lower than water ($\varepsilon \sim 81.4$), thereby providing a considerable dielectric constant contrast. The two-point sensor specific calibration procedure developed by *Sakaki et al.* [2008] and successfully used by *Camps-Roach et al.*

Table 1. Physical Properties of Fluids at 20°C

Fluid	Density (kg m^{-3})	Viscosity (Pa s^{-1})	Interfacial Tension With Water (N m^{-1})	Viscosity Ratio $\left(\frac{\mu^n}{\mu^w}\right)$
Water	999[a]	$1.12^{a} \times 10^{-3}$	–	–
Air	1.2[b]	$1.81^{b} \times 10^{-5}$	0.0681[b]	0.016
Silicone oil (0.65 cSt)	761[c]	$4.95^{c} \times 10^{-4}$	0.0378[d]	0.442
Silicone oil (5 cSt)	918[c]	$4.59^{c} \times 10^{-3}$	0.0378[d]	4.098

[a] *Munson et al.* [1990].
[b] *Chen et al.* [1999].
[c] Clearco, available at http://www.clearcoproducts.com.
[d] *Calabrese et al.* [1986].

[2010] was used to calibrate the EC-5 probes. The EC-5 probe readings were measured in completely silicone oil- and water-saturated columns for this study.

2.3. Static and Transient Drainage Experiments

[11] All of the experiments were performed without membranes, as some studies have suggested that the observed rate dependency in $(P_n - P_w) - S_w$ could be because of the presence of membranes [*Hassanizadeh et al.*, 2002; *Bottero*, 2009]. The columns were dry-packed and a stainless steel mesh (0.015 × 0.015 cm pore size) was placed at the lower and upper ends of the column to hold the sand in place. The pressure cell was flushed with CO_2 for 20 min followed by a slow (1 mL/min) upward displacement of the CO_2 with distilled, deionized, and de-aired water [*O'Carroll et al.*, 2005; *Camps-Roach et al.*, 2010]. Water was flushed for 24 h through the column before the permeability was quantified using the constant head method [*Klute and Dirksen*, 1986]. Water drainage experiments were initiated by applying a constant air pressure directly to the upper column boundary or by applying a constant air pressure above the silicone oil in the NAPL reservoir which was connected to the upper boundary of the column (Figure 1). Both air and silicone oil were injected vertically downward to avoid flow instabilities [*Das et al.*, 2007; *Camps-Roach et al.*, 2010]. In each experiment, water saturation, water pressure, nonwetting phase pressure, and fluid outflow were monitored every 15 s. All experiments were conducted at a controlled temperature of 22°C (±2°C).

[12] In the static experiments, air phase pressure, either applied directly to the upper column boundary or in the LNAPL reservoir, was increased in small increments (2–3 cm H_2O). Air or NAPL phase boundary pressure was increased only when outflow was near zero (i.e., an outflow rate of <0.2 g/hr). This process was repeated until only air or oil flowed out of the column. Dynamic experiments were conducted by applying a large air or silicone oil pressure in one step resulting in a rapid rate of change of saturation. An upper boundary air pressure step of 135 cm was applied in the air-water experiments and an air pressure of 85 cm was applied to the oil reservoir in the silicone oil-water experiments.

[13] Three experiments were conducted with air, one static and two dynamic experiments (upper boundary pressures of 120 and 135 cm). Six experiments were conducted with the 0.65 centistoke (cSt) silicone oil. Two of these experiments were conducted under static or slow desaturation rates. Four experiments were conducted at a fast desaturation rate, referred to as dynamic experiments, induced by imposing a constant air pressure of 85 cm H_2O. For the 5 cSt silicone oil-water system, two static and three dynamic experiments were conducted. Here, dynamic experiments were induced by applying a constant air pressure of 85 cm H_2O (the same as the 0.65 cSt oil). The maximum capillary numbers for these experiments were 1.4×10^{-9}, 3.4×10^{-10}, and 3.4×10^{-11} for the air, 0.65 cSt silicone oil and 5 cSt silicone oil-water systems, respectively, suggesting capillary forces were dominant. For this calculation the measured desaturation rate was used in conjunction with the distance between the EC-5 prongs as a representative length scale.

[14] In approximately half of the dynamic 0.65 cSt oil experiments, water entered the oil phase tensiometer during

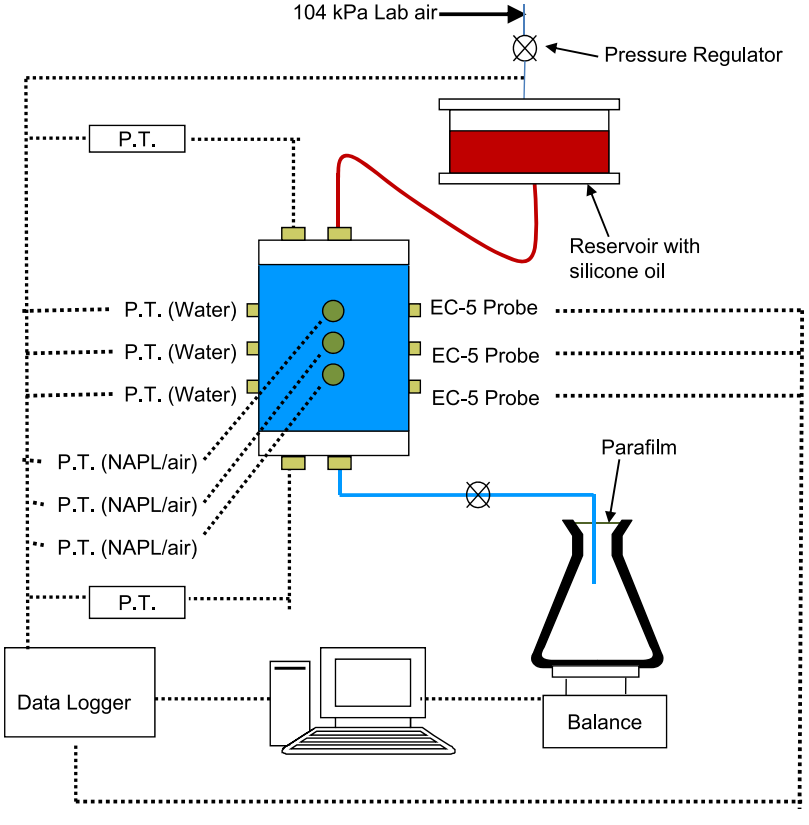

Figure 1. Experimental set up (P.T. = pressure transducer) modified from *Camps-Roach* [2008].

the experiment and these measurement locations could not be used. This may have been due to the volatility of this oil.

3. Results and Discussion

3.1. Effect of Boundary Conditions on Measured ($P_n - P_w$) − S_w Curves

[15] An initial set of static and dynamic air-water experiments were conducted to confirm the experimental procedure and compare results with those of a published study [*Camps-Roach et al.*, 2010]. $(P_n - P_w) - S_w$ is used as a general term describing both dynamic and equilibrium conditions whereas $P_c - S_w$ is a specific case only referring to equilibrium conditions (i.e., no flowing fluids). Under dynamic conditions the experimental apparatus cannot measure the capillary pressure operative at fluid/fluid/solid interface as there would be a pressure drop in a given fluid phase between the measurement location and the interface (e.g., due to viscosity). The equilibrium $(P_n - P_w) - S_w$ relationship is representative of conditions used in continuum-based models as it is typically assumed a priori that the rate dependency in $(P_n - P_w) - S_w$ can be neglected. $(P_n - P_w) - S_w$ results were similar for the static and dynamic experiments conducted at same upper boundary air pressure (i.e., 135 cm water) (Figure 2). This is expected as experimental conditions were the same in both studies. The dynamic experiments were conducted at two upper boundary air pressures (i.e., 120 and 135 cm water) in this study with $(P_n - P_w)$ data being lower, at the same water saturation, for the lower imposed air pressure experiment. These differences, however, are not statistically different. The static $P_c - S_w$ experiments conducted in this study were terminated prior to achieving residual water saturation as the data logger malfunctioned near the end of the experiment.

[16] For the silicone oil-water experiments porosity and permeability were similar, with normalized 95% confidence intervals of 0.16% and 1.42% for porosity and permeability, respectively (Table 2). The static experiments took up to 48 h to complete whereas the dynamic experiments were usually completed within 2 h, with the dynamic experiments conducted with the less viscous oil being quicker than those with the higher viscosity oil (e.g., Figure 3). Following an upper boundary oil phase pressure increase, water pressures increased immediately but quickly dissipated to hydrostatic pressure conditions before oil breakthrough. Oil phase pressure measurements at the three measurement locations increased monotonically following an upper boundary oil phase pressure step increase but the response time was longer than the response time for the water phase pressure tensiometers. Following oil breakthrough at the lower column boundary, both water and oil phase pressures fluctuated at all levels. Outflow rates were at maximum immediately after the pressure step and plateaued with time. At breakthrough, the slope of the cumulative outflow changes with time because of the lower specific gravity of oil when compared to water. Water saturation decreased sequentially from level 1 through 3 suggesting stable displacement of water in the column. In some instances, EC-5 moisture probes suggest that water saturation values were larger than 100% immediately at the initiation of the experiment. However, this increase was relatively small, with an observed maximum increase of 3%. To examine if a rate dependency was operative, as expected on the basis of equation (1), water saturation, if the static $P_c - S_w$ governed displacement, is plotted

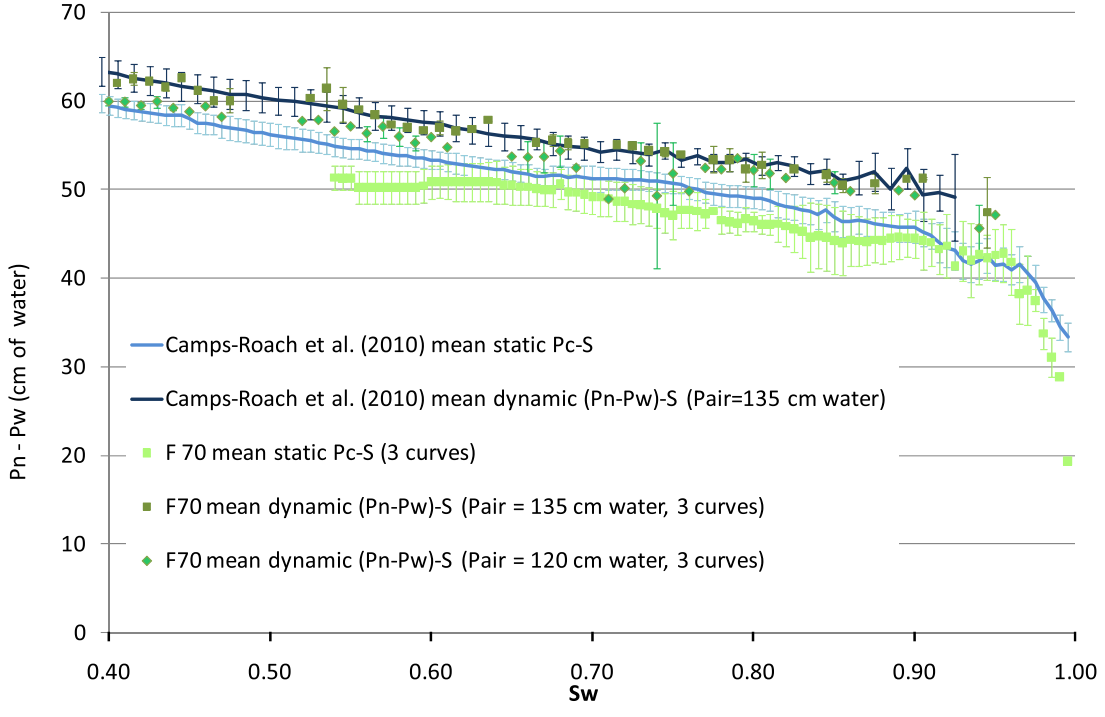

Figure 2. Mean of measured phase pressure difference-saturation curves for static and dynamic (pair = 135 cm) air-water experiments in addition to those reported by *Camps-Roach et al.* [2010] in the same experimental setup. Error bars indicate 95% confidence intervals about the mean.

Table 2. Summary of Oil-Water Experimental Results

Experiment Type	Porosity (ϕ)	Measurement Level for $P_c - S_w$	Permeability of Sand (m^2)	Total Pore Volume (cm^3)
0.65 cSt oil-water static 1	0.325	1, 2, and 3	1.42×10^{-11}	511.5
0.65 cSt oil-water static 2	0.324	1, 2, and 3	–	508.7
0.65 cSt oil-water dynamic 1	0.325	1 and 2	–	509.9
0.65 cSt oil-water dynamic 2	0.324	1	1.48×10^{-11}	509.3
0.65 cSt oil-water dynamic 3	0.325	1 and 3	1.45×10^{-11}	511.0
0.65 cSt oil-water dynamic 4	0.324	2 and 3	1.51×10^{-11}	508.4
5 cSt oil-water static 1	0.324	1, 2, and 3	–	509.1
5 cSt oil-water static 2	0.327	1, 2, and 3	–	513.9
5 cSt oil-water dynamic 1	0.325	1, 2, and 3	1.49×10^{-11}	510.9
5 cSt oil-water dynamic 2	0.324	1, 2, and 3	–	508.9
5 cSt oil-water dynamic 3	0.325	1, 2, and 3	1.53×10^{-11}	510.6
Mean	0.325	–	1.47×10^{-11}	510.2
Normalized 95% C.I.[a]	0.16	–	1.42	0.2

[a]Normalized 95% C.I. $= \frac{95\%\ C.I.}{Mean} \times 100$

on Figure 3. Water saturation is determined using the van Genuchten fit to static $P_c - S_w$ data and the measured phase pressure difference (e.g., NW1 – W1). This graph highlights differences in saturation breakthrough curves expected if the static $P_c - S_w$ curve is operative and those observed experimentally. At 50% water saturation this figure suggests that breakthrough is retarded ~24–28 min, which is much longer than the response times of the measurement devices (discussed below).

[17] The $(P_n - P_w) - S_w$ curves obtained for both oils under similar experimental conditions (i.e., static or dynamic) are similar (e.g., Figure 4). Furthermore, when these $(P_n - P_w) - S_w$ curves are scaled by interfacial tension using Leverett scaling they are very similar to the static air-water curves. In all cases the $(P_n - P_w) - S_w$ curves measured under dynamic primary drainage conditions are consistently higher than those measured under static primary drainage conditions. This is consistent with previous air-water experimental studies [*Camps-Roach et al.*, 2010; *Sakaki et al.*, 2010], in addition to the theoretical development of the rate dependence of $(P_n - P_w) - S_w$ [*Hassanizadeh and Gray*, 1990; *Kalaydjian*, 1992; *Hassanizadeh and*

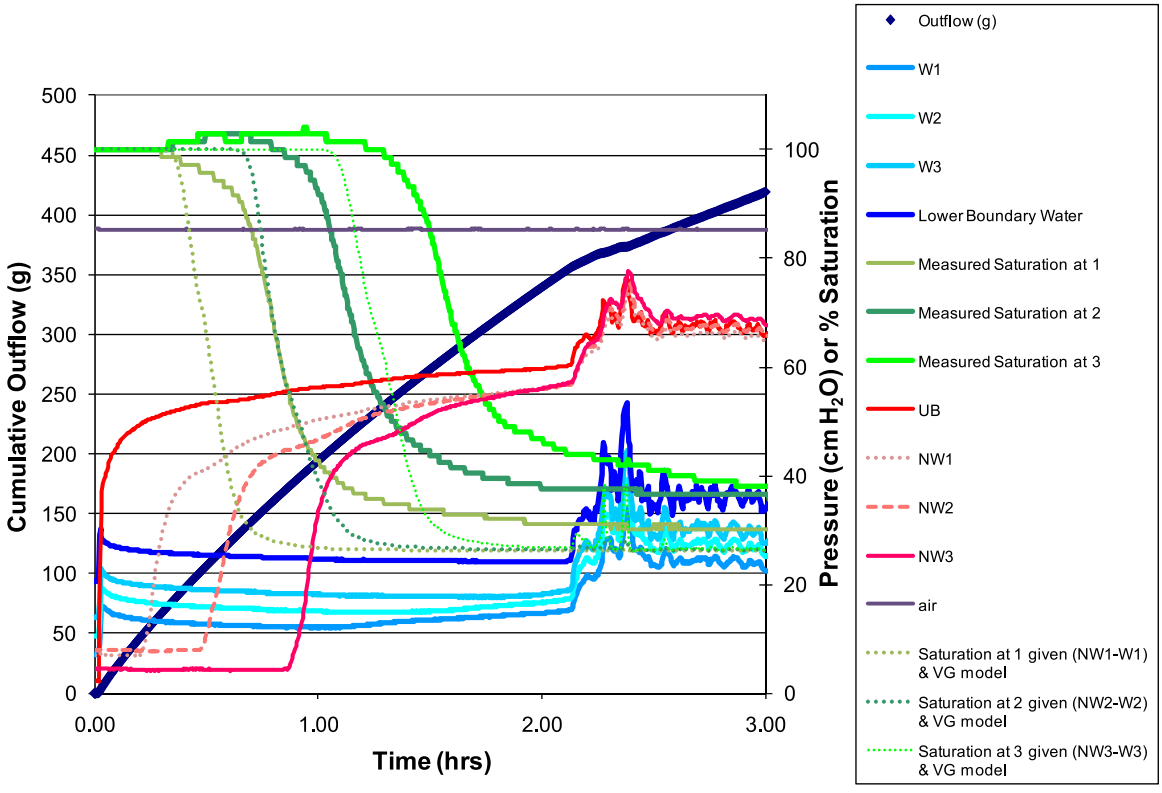

Figure 3. Measured experimental parameters at levels 1, 2, and 3 for 5 cSt silicone oil-water dynamic experiment 1 (pair = 85 cm): cumulative outflow, lower boundary pressure (LB), upper boundary pressure (UB), tensiometric oil pressures (NW1, NW2, and NW3), tensiometric water pressures (W1, W2, and W3), measured saturations, and saturations estimated given the pressure difference and the VG model versus time.

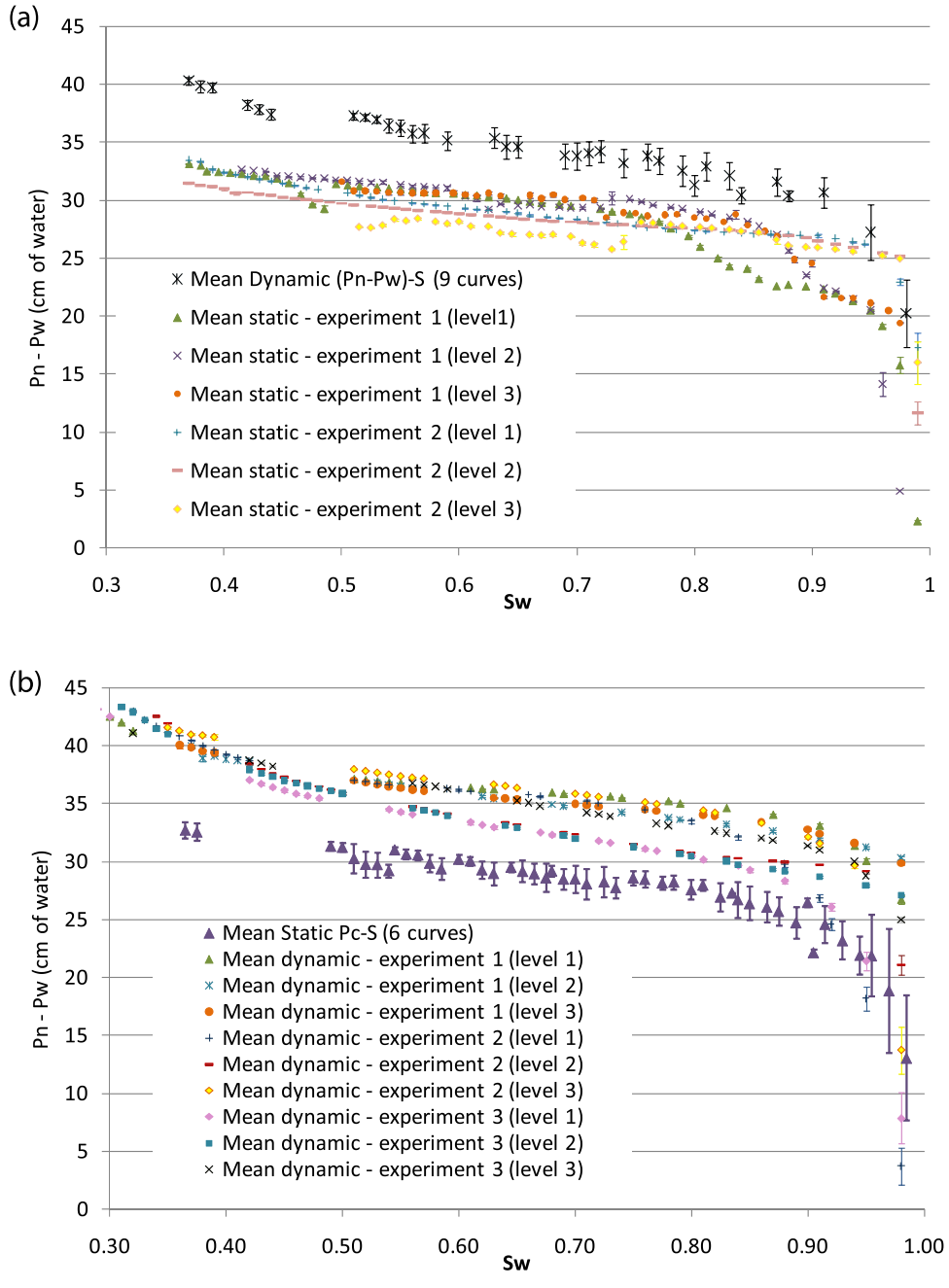

Figure 4. (a) Mean of all dynamic phase pressure difference-saturation experiments and mean of individual static phase pressure difference–saturation experiments and levels, including 95% C.I. about the mean, for 5 cSt silicone oil-water. (b) Mean of individual dynamic phase pressure difference–saturation experiments and levels as well as mean of all static phase pressure difference–saturation experiments, including 95% C.I. about the mean, for 5 cSt silicone oil-water.

Gray, 1993b, 1993a; *Hassanizadeh et al.*, 2002] and empirical relationships [*Stauffer*, 1978; *Barenblatt et al.*, 2003]. It was possible to quantify confidence intervals for the individual $(P_n - P_w) - S_w$ experiments at each measurement level, particularly for the static experiments, since measurements were logged at 15 s intervals for the entire experiment. As such, a large number of $(P_n - P_w) - S_w$ data points were obtained. In general, the confidence intervals were quite small (i.e., <0.2 cm water) at each level for these experiments. Averaging and confidence intervals for all data obtained under similar conditions will be discussed in section 3.2.

[18] A series of tests were conducted to quantify any lag in device measurement times as this could be important in the quantification of the rate dependence of $(P_n - P_w) - S_w$. In the first test the column was completely filled with 0.65 cSt silicone oil (i.e., no sand) with the pores of the nonwetting phase ceramic cups and Teflon-FEP tubing connecting the cups to the pressure transducers completely saturated with silicone oil. When the oil was pressurized the

pressure transducers responded to 90% of their steady state value within 45 s (results not shown). This delayed response time could be because of the finite time for pressure to be transferred through the ceramic cups or because of the compressibility of the oil. Increased conductance of the ceramic cups would increase the response time of the tensiometers as suggested in the work by *Selker et al.* [1992] who discussed the contribution of soil hydraulic conductivity and cup conductance to tensiometer response times. Care would have to be taken not to reduce the entry pressure of the ceramic cup to the fluid phase that does not wet the cup by increasing the ceramic cup conductance. An additional set of tests was conducted to evaluate wetting and nonwetting phase tensiometer response times in partially water-saturated porous media. In the partially saturated experiments the water outflow line at the base of the column was closed, the oil pressure was increased, and the pressure transducer response time monitored at the three levels as well as at the top and base of the column. Water pressure readings at all levels increased to more than 60% and 90% of their steady state values in ~60 and 210 s, respectively. The oil pressure readings generally increased to 60% and 90% of their steady state value in approximately 165 and 400 s at all levels, respectively. Any delay in nonwetting phase tensiometers results in reported ($P_n - P_w$) less than the actual ($P_n - P_w$) value. At the start of the experiment, the air inflow valve was opened immediately before the water effluent valve was opened. In this very small time, increment wetting phase pressure increased in the column and then slowly decreased. As such, any delay in wetting phase tensiometer response time, due to the finite time for the pressure signal to travel through the low permeability ceramic cups, would serve to decrease measured ($P_n - P_w$) below its actual value. This sensitivity analysis suggests that any tensiometer delay would serve to decrease ($P_n - P_w$) below their actual value (i.e., tensiometer lag would decrease any rate dependency). For the soil moisture probes, a recent literature study suggests that they respond much quicker than the tensiometers [*Sakaki et al.*, 2010]. As such, their response time will not impact observed results.

[19] A key assumption in this study is that water saturation and phase pressures are measured at the same location and over the same measurement scale. Literature studies suggest that the orientation of the soil moisture prongs does impact measurement sensitivity [e.g., *Roth et al.*, 1990]. To assess this issue, independent quantification of the region over which the EC-5 probes measure saturation was completed. This analysis suggests that they are most sensitive between the top of the upper prong and the bottom of the lower prong (i.e., a vertical distance of 1.5 cm). The ceramic cups have a diameter of 0.64 cm, however, they likely sense pressure in a slightly larger area. Nonetheless, the measurement scale for water saturation is larger than that of the ceramic cups, however, both are centered at the same location. This relatively small measurement scale difference is assumed to not impact reported results.

3.2. Determination of 95% Confidence Interval on ($P_n - P_w$) − S_w Curves

[20] Six static and seven dynamic ($P_n - P_w$) − S_w curves were obtained for the 0.65 cSt oil-water system. Similarly, six static and nine dynamic ($P_n - P_w$) − S_w curves were obtained for the 5 cSt oil-water system. To facilitate a statistical comparison of the static and dynamic ($P_n - P_w$) − S_w curves and determine if imposed boundary condition impacted the ($P_n - P_w$) − S_w curve, the mean and 95% confidence intervals about the mean ($P_n - P_w$) − S_w curves were quantified [*Camps-Roach et al.*, 2010; *Sakaki et al.*, 2010]. To do this the mean phase pressure difference at a given water saturation was calculated for each level for each experiment (i.e., for some experiments multiple-phase pressure differences were sometimes measured at a given saturation, particularly for the slower static experiments). Water saturations were then divided into 0.5% and 1% intervals for static and dynamic experiments, respectively. The mean phase pressure difference at each individual level and experiment were then averaged for a given saturation range for experiments with similar boundary conditions. As such, the 95% confidence interval of averaged-phase pressure differences could then be calculated for each experiment type (i.e., static and dynamic). Data are only reported when there are at least three data points in a given saturation bin.

[21] The mean static and mean dynamic ($P_n - P_w$) − S_w curves were statistically different for both the 0.65 and 5 cSt oil-water experiments (Figures 5 and 6). These differences suggest that the magnitude of the measured ($P_n - P_w$) − S_w curves was dependent on boundary/desaturation conditions consistent with other experimental and theoretical studies [*Kalaydjian*, 1992; *Hassanizadeh and Gray*, 1993a; *Hassanizadeh et al.*, 2002].

3.3. Determination of Capillarity Coefficient (τ) and Its Dependence on Wetting Fluid Saturation (S_w)

[22] The capillarity coefficient (τ) was calculated using equation (1). To do this, ($P_n - P_w$), quantified for both static and dynamic conditions, as well as the rate of water saturation change, was required at a given saturation. The van-Genuchten function [*van Genuchten*, 1980] was therefore fitted to mean static $P_c - S_w$ curves for both 0.65 and 5 cSt oil-water systems as well as the air-water system. The van Genuchten function was selected as it closely matched mean static curves (Figures 5 and 6). Fitted van Genuchten parameters values are given in Table 3. The phase pressure difference at equilibrium corresponding to the water saturation, at which ($P_n - P_w$) was quantified in the dynamic experiments, was determined using the van Genuchten model fit. The water desaturation rate was quantified for each dynamic experiment using a seven point moving polynomial smoothing routine [*Golay*, 1972]. The maximum desaturation rate for the 5 cSt oil-water system (9.8×10^{-4} s^{-1}) was smaller than that for the 0.65 cSt oil-water system (2.9×10^{-3} s^{-1}) as expected due to the viscosity difference. It is important to distinguish between actual water saturation decreases and decreases due to noise in the EC-5 probes. The stability of the EC-5 probes was therefore assessed at different degrees of saturation when the column was at equilibrium (i.e., when the outflow valve was closed). To do this, between 120 and 150 water saturations readings were collected at a given degree of saturation. The maximum 95% confidence interval about the mean water saturation was 0.12%, which was used as the experimental detection limit of the EC-5 soil moisture probes. If measured

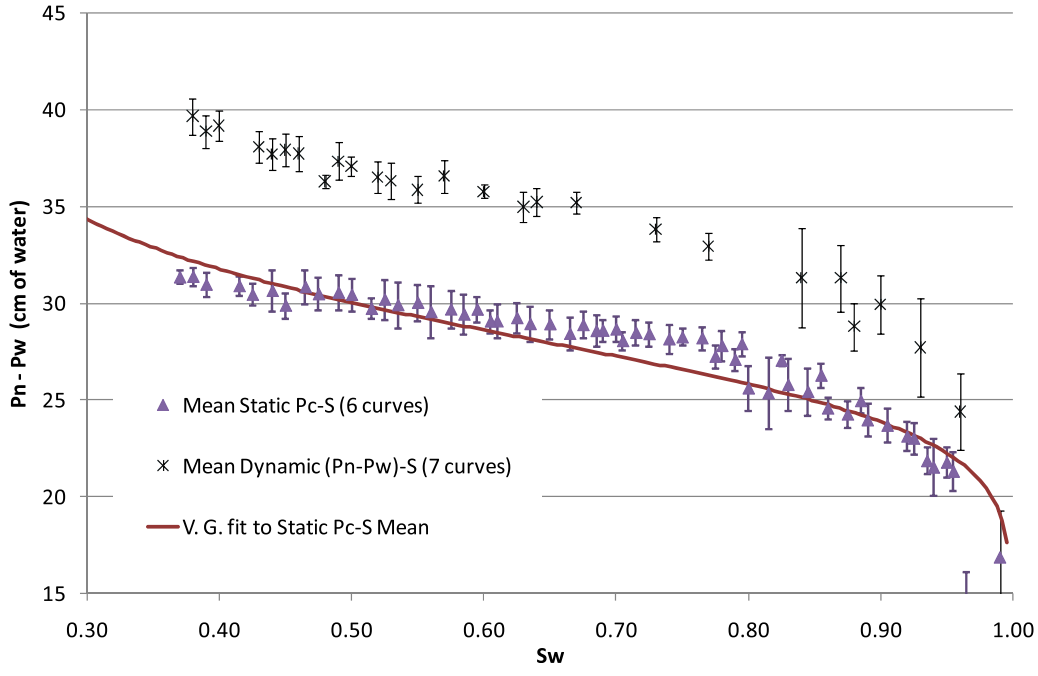

Figure 5. Comparison of the 0.65 cSt oil-water mean static and mean dynamic phase pressure difference-saturation curves. Error bars indicate the 95% confidence intervals about the mean.

water saturation decrease was less than this detection limit the capillarity coefficient was not quantified.

[23] The capillarity coefficient, τ, was averaged over a 2% water saturation interval for a given fluid pair to facilitate a statistical comparison between capillarity coefficients (Figure 7). The magnitude of τ for the 5 cSt silicone oil-water system is generally higher than that for the 0.65 cSt oil-water and air-water systems. This is the first experimental study to observe that the capillarity coefficient is statistically different for NAPLs of different viscosities. τ was similar for the air-water and 0.65 cSt oil-water systems above a water saturation of 50%. This is likely because of similar effective viscosities, particularly at high water saturations, as will be discussed later. In all cases, τ is constant

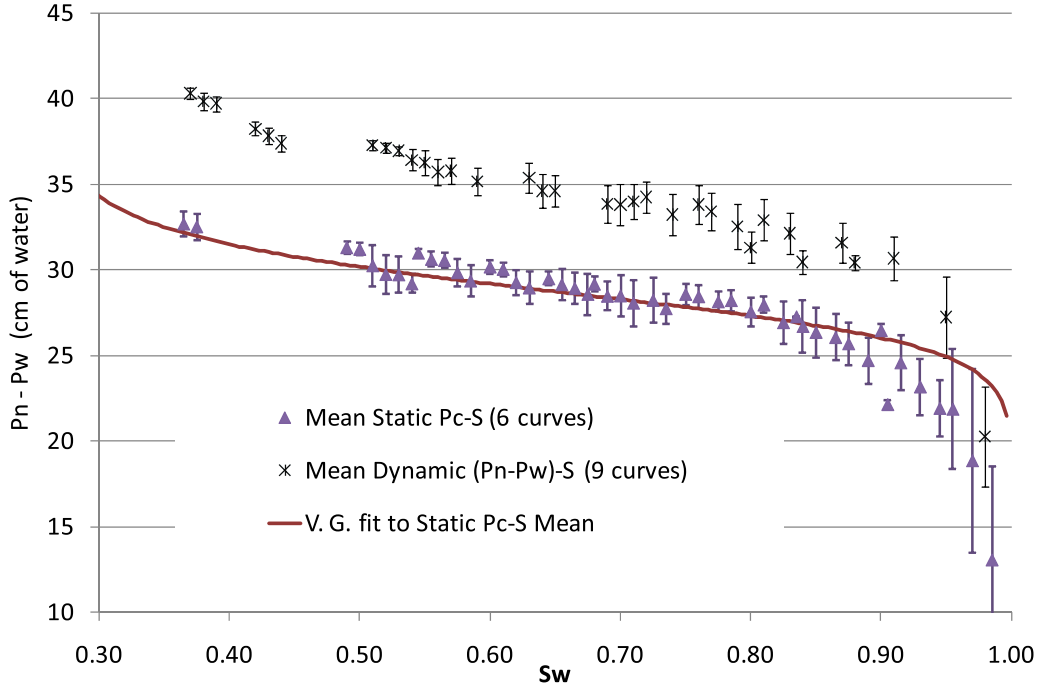

Figure 6. Comparison of the 5 cSt oil-water mean static and mean dynamic phase pressure difference-saturation curves. Error bars indicate the 95% confidence intervals about the mean.

Table 3. Fitted van-Genuchten Static $P_c - S_w$ Parameters for Different Fluid Pairs

Fluid Pairs	α (cm^{-1})	n	S_{rw}
Air -Water[a]	1.87×10^{-2}	11	0.15
0.65 cSt Silicone oil-water	3.57×10^{-2}	11	0.18
5 cSt Silicone oil-water	3.49×10^{-2}	18	0.26

[a]*Camps-Roach* [2008]

between 70% and 90% water saturation and increases as water saturation decreases below 60% for the silicone oil-water systems. For the 5 cSt oil, τ varies between 2.74×10^6 and 1.2×10^6 kg/m^{-1}/s^{-1} while for the 0.65 cSt oil, τ varies between 2.16×10^6 and 4.85×10^5 kg/m^{-1}/s^{-1}. This range is consistent with published PCE-water and oil-water studies [*Kalaydjian*, 1992; *Manthey et al.*, 2005; *O'Carroll et al.*, 2005; *Berentsen et al.*, 2006; *Bottero et al.*, 2006; *Das et al.*, 2007; *Bottero*, 2009; *Joekar-Niasar et al.*, 2010]. For example, τ ranged between 5.4×10^5 and 2.9×10^6 kg/m^{-1}/s^{-1} for 1.44 cSt oil-water experiments in sandstone and limestone [*Kalaydjian*, 1992]. The permeability of the permeable media in this literature study was approximately two orders of magnitude smaller than the permeability of the sand used in this study making direct comparison difficult. *Bottero et al.* [2006, 2009] and *Manthey* [2006], using a similar experimental setup, found that τ ranged between 10^5 to 10^6 kg/m^{-1}/s^{-1} for PCE-water experiments conducted in a fine sand. Their sand was nearly an order of magnitude less permeable than the porous media used in this study. These experimental studies, however, did not investigate the impact of viscosity on the magnitude of the capillarity coefficient. Use of the *Stauffer* [1978] equation, modified for effective viscosity, yields τ ranging from 4.34×10^4, 3.80×10^4, and 1.35×10^5 kg/m^{-1}/s^{-1} in completely water-saturated porous media in 5 and 0.65 cSt oil-water and air-water systems, respectively. At the lowest water saturations where τ is reported, τ ranged from 1.18×10^5, 2.64×10^4, and 3.92×10^4 kg/m^{-1}/s^{-1} in 5 and 0.65 cSt oil-water and air-water systems, respectively, using the *Stauffer* [1978] equation. Use of the effective viscosity-modified Stauffer equation yields τ estimates that are relatively insensitive to viscosity for the 0.65 cSt oil-water system as the viscosity of both fluid pairs are similar. For the other two systems (i.e., 5 cSt oil-water and air-water system) τ estimates are a stronger function of saturation because of the larger difference in viscosities for these fluid pairs. Finally, this analysis suggests that τ estimates using the *Stauffer* [1978] equation are approximately an order of magnitude less than those observed in this study, suggesting that further work is required to develop a predictive relationships for τ. It is noted that the study by *Camps-Roach et al.* [2010] found that the Stauffer equation [*Stauffer*, 1978] accounted for the general trend of increased capillarity coefficient with decreased sand permeability but the magnitude of differences were different, consistent with this study.

[24] As discussed in the introduction, numerical studies [*Manthey*, 2006; *Das et al.*, 2007; *Gielen*, 2007; *Joekar-Niasar et al.*, 2010] have explored the effect of fluid viscosity on the magnitude of τ and have reported contradictory results. The models, based on continuum scale modeling [*Manthey*, 2006; *Das et al.*, 2007], do not incorporate interfacial dynamics and attribute the observed rate dependence of $(P_n - P_w) - S_w$ to upscaling. In this experimental study, the observed rate dependence of $(P_n - P_w) - S_w$ is not attributed to upscaling as the rate dependency is quantified at the REV scale. As suggested by *Dahle et al.* [2005],

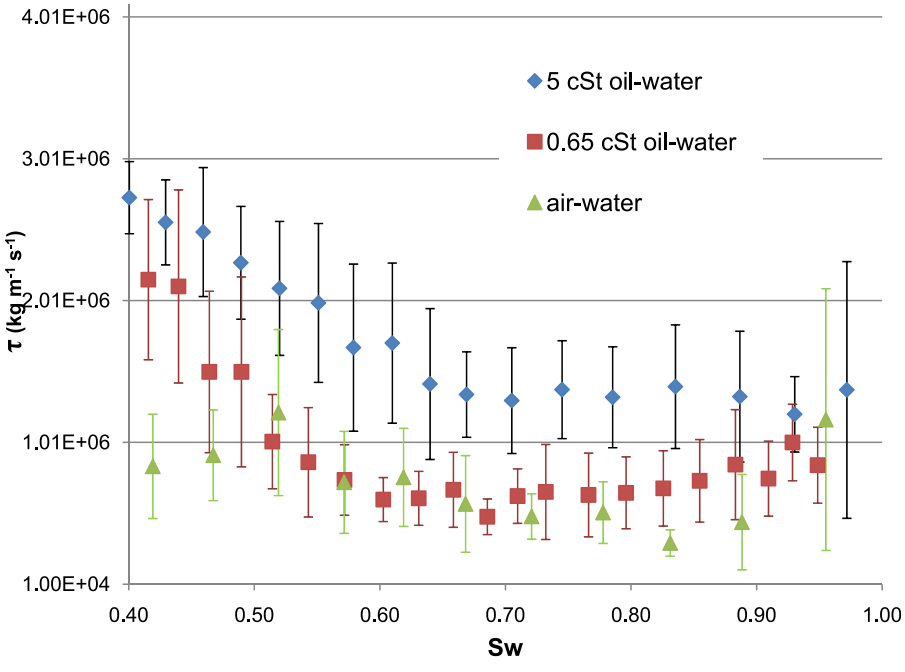

Figure 7. Comparison of the dynamic coefficient (τ) versus wetting phase saturation (Sw) for 5 and 0.65 cSt silicone oil-water dynamic experiments (constant air pressure of 85 cm) and air-water dynamic experiments (upper boundary air pressure = 135 cm).

viscosity impacts the fluid–fluid interface and should therefore be included in models. This has been partially addressed by *Joekar-Niasar et al.* [2010] and *Joekar-Niasar and Hassanizadeh* [2011] using a pore network approach. Their approach implicitly assumes that the equilibrium capillary pressure-saturation relationship is appropriate at the pore scale under both static and dynamic conditions. They postulate that rearrangement of fluid–fluid interfaces over their averaging volume is a function of viscosity and larger viscosity ratios will delay the rearrangement process. To account for viscosity, they normalized the capillarity coefficient by the effective fluid viscosity. Using this approach the capillarity coefficients quantified for the three fluid pairs investigated in this study collapsed and were statistically equivalent for effective water saturations larger than 50%, with values ranging between 5×10^8 and 10^9 (Figure 8). Normalization of the capillarity coefficient by the mobility ratio, as has been suggested by *Das et al.* [2007], was also assessed using the Brooks-Corey/Burdine relative permeability model. This normalization procedure did not collapse capillarity coefficients together and the normalized capillarity coefficients were still a strong function of saturation (Figure 9). Use of alternate relative permeability models (i.e., Brooks-Corey/Mualem; van Genuchten/Burdine; van Genuchten/Mualem) did not improve this normalization procedure. Although further work is required for a broader range of fluid pairs, normalization using effective viscosity suggests that normalization approaches may be able to account for some of the range of capillarity coefficients reported in the literature. For example, the Stauffer equation [*Stauffer*, 1978] or the dynamic number [*Manthey et al.*, 2008], modified to account for effective viscosity and relative permeability as will be discussed in section 3.4, could be used as starting points.

3.4. Estimation of Governing Forces

[25] In order to assess the relative importance of the forces governing multiphase flow, *Manthey et al.* [2008] conducted a dimensional analysis of the multiphase flow equations. The analysis resulted in two important dimensionless parameters, namely the dynamic number (Dy) and dynamic capillary number (DyC). The Dy refers to the ratio of dynamic forces to viscous forces while DyC refers to the ratio of dynamic forces to equilibrium capillary forces. One goal of this analysis would be to determine criterion when dynamic effects may be important, similar to the phase diagram by *Lenormand et al.* [1988] as related to stable fluid displacement. The expressions by *Manthey et al.* [2008] have been modified herein to include effective viscosity and the dynamic coefficient as a function of water saturation:

$$\mathrm{Dy} = \frac{k\,\tau(S_w)}{\mu_{eff} l_c^2 \phi}, \tag{4}$$

$$\mathrm{DyC} = \frac{u_c \tau(S_w)}{P_{cc} l_c \phi}, \tag{5}$$

where, l_c is a characteristic length, u_c is a characteristic velocity, P_{cc} is a characteristic capillary pressure. Similar to the approach by *Camps-Roach et al.* [2010], l_c was taken as the distance between the two prongs of the EC-5 probe. *Manthey et al.* [2008] suggested that the front width was an appropriate characteristic length selection. As such, the distance between the two prongs assumes that this is a reasonable estimate of the front width. P_{cc} was taken as the entry pressure and u_c/l_c was the maximum observed desaturation rate.

[26] As expected, the dynamic number is relatively constant with the water saturation given the discussion related

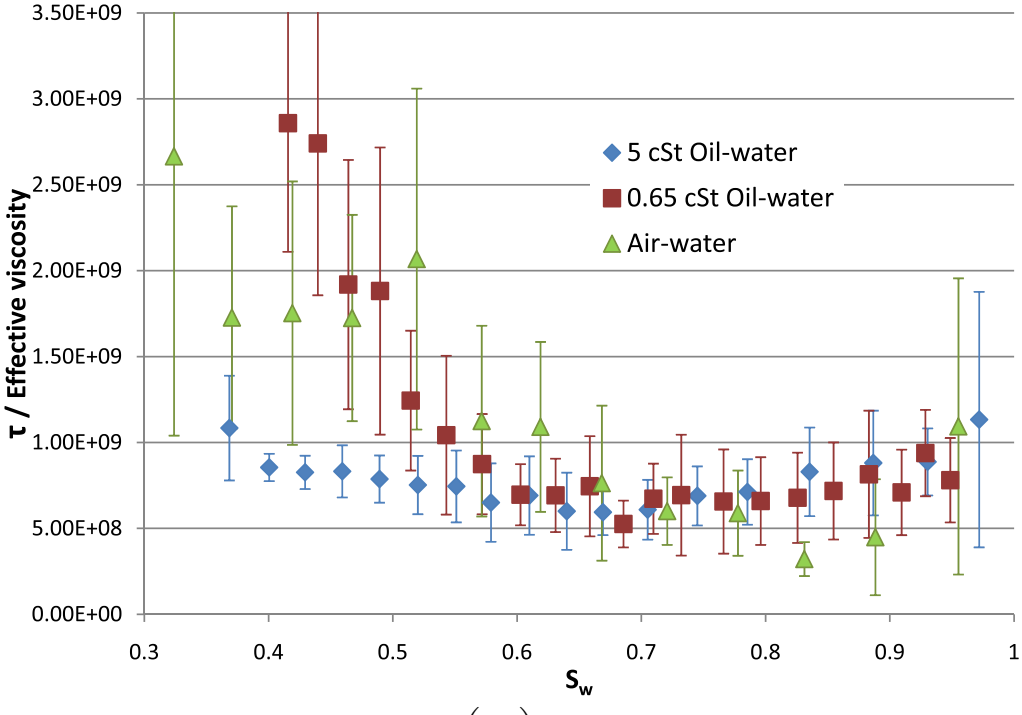

Figure 8. Normalized dynamic coefficient $\left(\frac{\tau}{\mu_{eff}}\right)$ for 5 and 0.65 cSt silicone oil-water dynamic experiments and air-water dynamic experiments.

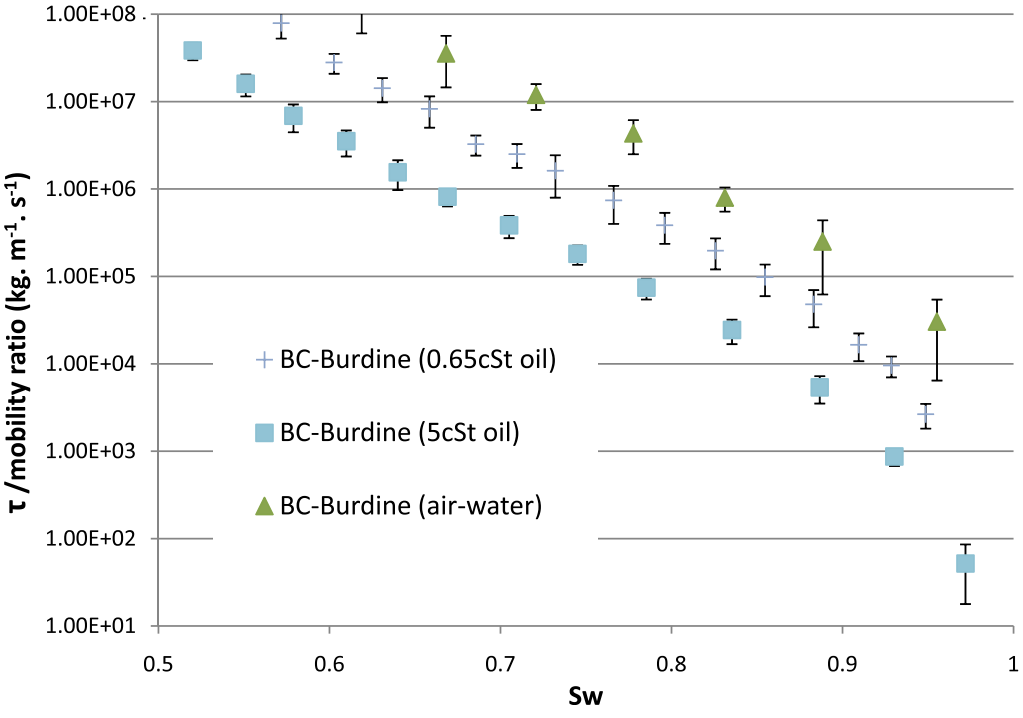

Figure 9. Normalized dynamic coefficient $\tau \Big/ \frac{k_{rw}\,\mu^n}{k_{rn}\,\mu^w}$ for 5 and 0.65 cSt silicone oil-water dynamic experiments and air-water dynamic experiments using the Brooks-Corey/Burdine relative permeability relationship.

to normalizing the dynamic coefficient by effective viscosity (Figure 10). The dynamic number generally ranges between 200 and 500 for all systems above water saturations of 50% and then increases with decreasing water saturation. This is in the range of the dynamic number reported by *Camps-Roach et al.* [2010] (Dy = 410) using the same sand with air and water as the fluids. It should be noted that they used water viscosity in their calculations and not effective viscosity. The dynamic capillary numbers range between 1 and 7 and generally increase as water saturation decreases to below 60%, as expected, given the trend of the dynamic coefficient with decreasing water saturation (Figure 10). The numerator in the dynamic capillary number is the same as the right-hand side of equation (1) (i.e., assuming $u_c/l_c = \partial S_w/\partial t$) and the characteristic capillary pressure is on the same order of magnitude as P_c^s. As such, equations (1) and (5) are not independent. These dynamic numbers are larger than that reported by *Camps-Roach et al.* [2010] (DyC = 1.4). The dynamic capillary pressure number includes a characteristic velocity term. Here the maximum desaturation rate was used in the calculations, which is not a function of saturation. Alternatively, the desaturation rate that varies with saturation could be used in these calculations. However, this would essentially be a plot of $([P_n - P_w] - P_c^s)$, multiplied by constants, versus water saturation. A broader range of experiments is needed in the transition between when the equilibrium assumption is appropriate and when the rate dependency is operative (e.g., a broader range of desaturation rates, viscosity ratios, and soil permeability). Results from *Camps-Roach et al.* [2010] suggests that $\tau(S_w)$ is larger for finer textured soils, however, the dynamic number was larger for the coarser soil used in their study. In their study they assumed a constant τ and fluid viscosity. Reevaluation of their data using $\tau(S_w)$, effective viscosity, and relative permeability multiplied by the intrinsic permeability yields dynamic numbers that decrease with water saturation, to approximately $S_w = 0.9$, and are then relatively constant with water saturation (Figure 11). Dynamic numbers are larger for the coarser sand above $S_w = 0.9$ and are then similar at ~150. Further work is required to determine if this difference is statistical. This analysis of a limited data set suggests that the dynamic number may be an effective means of normalizing observed capillarity effects.

4. Summary and Conclusion

[27] A number of air-water and oil-water primary drainage experiments were conducted in a single, homogeneous porous medium with two silicone oils with different viscosities. The pressures and saturations of the two immiscible phases were quantified inside the sand column at three elevations in a measurement depth of ~1 cm. The response time of the soil moisture probes was much faster than the tensiometers. A sensitivity analysis suggests that any delay in tensiometer response would decrease the observed rate dependency in $(P_n - P_w)$ below what was actually operative. Ninety-five percent confidence intervals on $(P_n - P_w) - S_w$ curves confirmed that the $(P_n - P_w) - S_w$ curve measured under dynamic conditions was statistically different than those obtained under static conditions. Experiments conducted in this study did not use hydrophobic and hydrophilic membranes, as it has been suggested that their presence may influence the $(P_n - P_w) - S_w$ curve [*Bottero et al.*, 2006; *Bottero*, 2009].

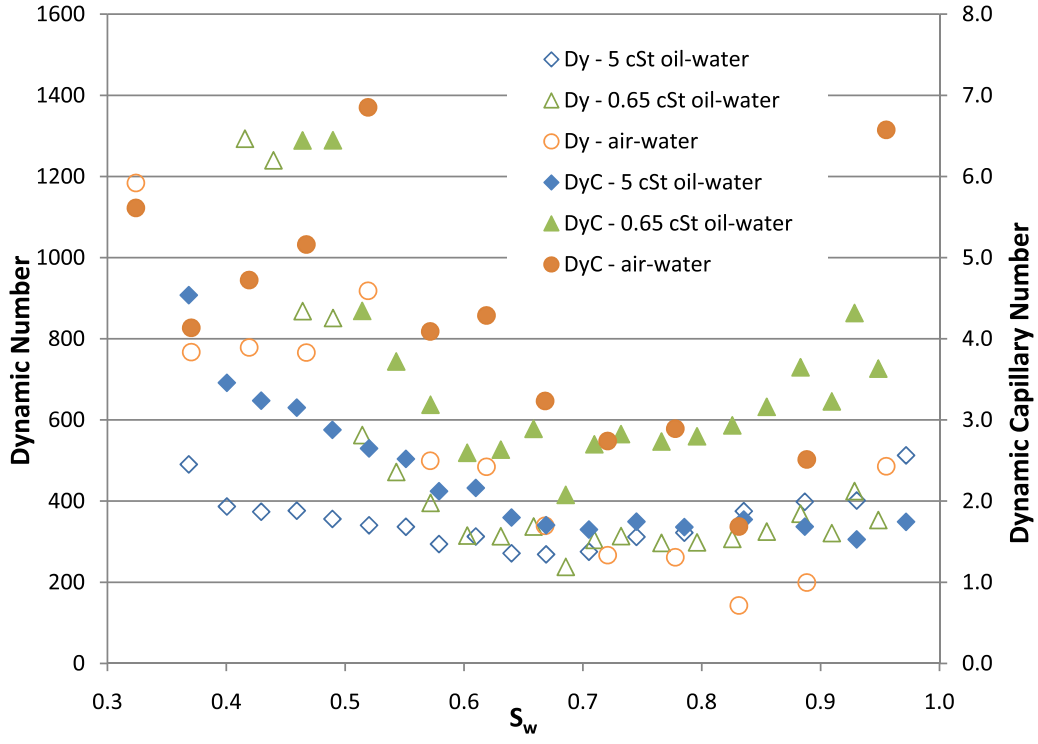

Figure 10. Dynamic and dynamic capillary number for 5 and 0.65 cSt silicone oil-water and air-water dynamic experiments.

[28] To the authors' knowledge, this study is the first to experimentally demonstrate that the capillarity coefficient is statistically different for NAPLs with different fluid viscosities. The capillarity coefficient decreased for NAPLs with smaller nonwetting fluid viscosity (i.e., 5 cSt oil-water, followed by 0.65 cSt oil-water). This analysis assumes that the oil densities are similar enough (i.e., a difference of 20%) and any differences in the capillarity coefficient is because of viscosity differences. τ values that were normalized by effective viscosity [*Joekar-Niasar and Hassanizadeh*, 2011] collapsed, and found to be statistically equivalent above a water saturation of 50% indicating that normalization approaches may be able to account for some of the range of capillarity coefficients reported in the literature. The magnitude of the capillarity coefficient observed in this study is within the range reported in the literature. Further work is required to investigate additional factors that can contribute to the rate dependency in $(P_n - P_w) - S_w$ (interfacial phenomena (i.e., contact angle and wettability), micro scale heterogeneity, and domain size). These results have significant implications related to simulating multiphase flow scenarios in the subsurface (e.g., NAPL migration and CO_2 sequestration). Modeling tools used to simulate multiphase flow should incorporate the rate dependency in $(P_n - P_w) - S_w$, particularly when fluid saturations are changing rapidly.

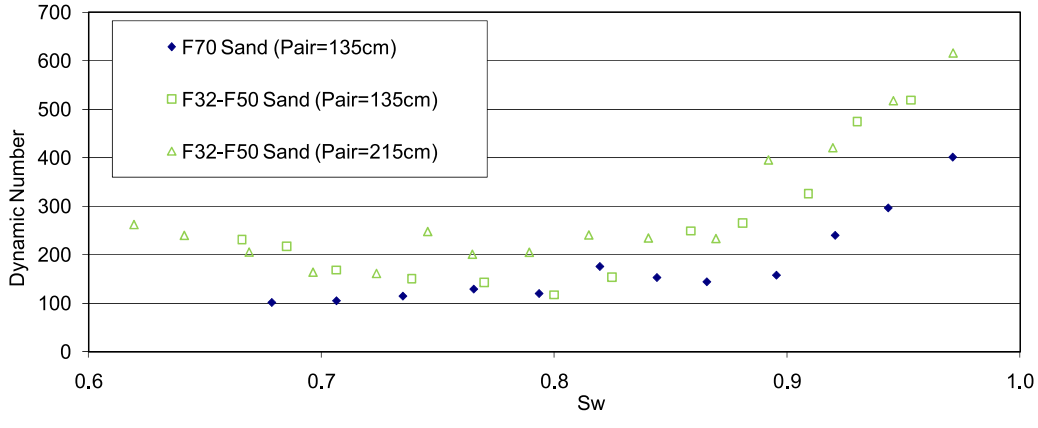

Figure 11. Dynamic number for data of air/water experimental data of *Camps-Roach et al.* [2010], reevaluated using $\tau(S_w)$, effective viscosity, and relative permeability multiplied by instrinsic permeability.

[29] **Acknowledgments.** This research was supported by Natural Sciences and Engineering Research Council (NSERC) of Canada and Canadian Foundation for Innovation grants. The authors would also like to thank Kristina Nangle for her careful assessment of EC-5 sensitivity.

References

Barenblatt, G. I. (1971), Filtration of two nonmixing fluids in a homogeneous porous medium, *Sov. Acad. Izvestia, Mechanics of Gas and Fluids*, *5*, 857–864.

Barenblatt, G. I., T. W. Patzek, and D. B. Silin (2003), The mathematical model of nonequilibrium effects in water-oil displacement, *SPE J.*, *8*(4), 409–416.

Berentsen, C. W. J., S. M. Hassanizadeh, A. Bezuijen, and O. Oung (2006), Modelling of two-phase flow in porous media Including non-equilibrium capillary pressure effects, in XVI International Conference on Computational Methods in Water Resources, Copenhagen, Denmark.

Bogena, H. R., J. A. Huisman, C. Oberdorster, and H. Vereecken (2007), Evaluation of a low-cost soil water content sensor for wireless network applications, *J. Hydrol.*, *344*(1–2), 32–42.

Bottero, S. (2009), *Advances in the Theory of Capillarity in Porous Media*, 201 pp., Utrecht University, Netherlands.

Bottero, S., S. M. Hassanizadeh, P. J. Kleingeld, and A. Bezuijen (2006), Experimental Study of Dynamic Capillary Pressure Effects in Two-Phase Flow in Porous Media, in XVI International Conference on Computational Methods in Water Resources, www.cmwr-xvi.org, Copenhagen, Denmark.

Brooks, R. H., and A. T. Corey (1964), Hydraulic properties of porous media, in Hydrol. pap. 3, Colo. State Univ., Fort Collins, CO.

Busby, R. D., R. J. Lenhard, and D. E. Rolston (1995), An investigation of saturation-capillary pressure relations in two- and three-fluid systems for several NAPLS in different porous media, *Ground Water*, *33*, 570–578.

Calabrese, R. V., T. P. K. Chang, and P. T. Dang (1986), Drop breakup in turbulent stirred-tank contactors. 1. *Effect of dispersed-phase viscosity, AIChE J.*, *32*(4), 657–666.

Camps-Roach, G. W. (2008), Investigating The Transient Effects of Two-Phase Flow in Porous Media, Monograph thesis, 148 pp., University of Western Ontario, London.

Camps-Roach, G., D. M. O'Carroll, T. A. Newson, T. Sakaki, and T. H. Illangasekare (2010), Experimental investigation of dynamic effects in capillary pressure: Grain size dependency and upscaling, *Water Resour. Res.*, *46*, W08544, doi:10.1029/2009WR008881.

Chen, J., J. W. Hopmans, and M. E. Grismer (1999), Parameter estimation of two fluid capillary pressure-saturation and permeability functions, *Adv. Water Resour.*, *22*, 479–493, doi:10.1016/S0309-17-9(98)00025-6.

Clearco (2010), Pure Silicone Fluids, available at http://www.clearcoproducts.com, Bensalem, PA.

Czarnomski, N. G., T. Moore, J. L. Pypker, and B. Bond (2005), Precision and accuracy of three alternative instruments for measuring soil water content in two forest soils of the Pacific Northwest Can., *J. For. Res.*, *35*(8), 1867–1876.

Dahle, H. K., M. A. Celia, and S. M. Hassanizadeh (2005), Bundle-of-tubes model for calculating dynamic effects in the capillary-pressure-saturation relationship, *Transp. Porous Media*, *58*(1–2), 5–22.

Das, D. B., R. Gauldie, and M. Mirzaei (2007), Dynamic effects for two-phase flow in porous media: Fluid property effects, *AIChE J.*, *53*(10), 2505–2520.

Friedman, S. P. (1999), Dynamic contact angle explanation of flow rate-dependent saturation-pressure relationships during transient liquid flow in unsaturated porous media, *J. Adhesion Sci. Technol.*, *13*(12), 1495–1518.

Gielen, T. W. J. (2007), Dynamic effects in two-phase flow in porous media: a pore scale network approach, PhD Dissertation thesis, 183 pp., Delft University of Technology, Delft, Netherlands.

Golay, M. J. E. (1972), Smoothing of data by least-squares procedures and by filtering, *IEEE Trans. Comput.*, *C-21*(3), 299–301.

Gray, W. G., and S. M. Hassanizadeh (1991a), Paradoxes and realities in unsaturated flow theory, *Water Resour. Res.*, *27*(8), 1847–1854, doi:10.1029/91WR01259.

Gray, W. G., and S. M. Hassanizadeh (1991b), Unsaturated flow theory including interfacial phenomena, *Water Resour. Res.*, *27*(8), 1855–1863, doi:10.1029/91WR01260.

Hassanizadeh, S. M., and W. G. Gray (1990), Mechanics and thermodynamics of multiphase flow in porous-media including interphase boundaries, *Adv. Water Resour.*, *13*(4), 169–186.

Hassanizadeh, S. M., and W. G. Gray. (1993a), Toward an improved description of the physics of 2-phase flow, *Adv. Water Resour.*, *16*(1), 53–67.

Hassanizadeh, S. M., and W. G. Gray (1993b), Thermodynamic basis of capillary-pressure in porous-media, *Water Resour. Res.*, *29*(10), 3389–3405, doi:10.1029/93WR01495.

Hassanizadeh, S. M., M. A. Celia, and H. K. Dahle (2002), Dynamic effect in the capillary pressure-saturation relationship and its impacts on unsaturated flow, *Vadose Zone J.*, *1*(1), 38–57.

Hopmans, J. W., M. E. Grismer, and J. Chen (1998), Parameter estimation of two-fluid capillary pressure—saturation and permeability functions, Univ. California, Davis.

Joekar-Niasar, V., and S. M. Hassanizadeh (2011), Effect of fluids properties on non-equilibrium capillarity effects; dynamic pore-network modelling, *Int. J. Multiphase Flow*, *37*, 198–214.

Joekar-Niasar, V., S. M. Hassanizadeh, and H. K. Dahle (2010), Non-equilibrium effects in capillarity and interfacial area in two-phase flow: Dynamic pore-network modelling, *J. Fluid. Mech.*, *655*, 38–71.

Kalaydjian, F. J.-M. (1992), Dynamic Capillary Pressure Curve for Water/Oil Displacement in Porous Media: Theory vs. Experiment, paper presented at 67th SPE Annual Technical Conference and Exhibition, Society of Petroleum Engineers Inc., Washington, D.C., 4–7 October 1992.

Klute, A., and C. Dirksen (1986), Hydraulic Conductivity and Diffusivity: Laboratory Methods: Methods of Soil Analysis, Part 1, Physical and Mineralogical Methods-Agronomy Monograph no. 9 (2nd Edition).

Lenhard, R. J., and J. C. Parker (1987), Measurement and prediction of saturation-pressure relationships in three-phase porous media systems, *J. Contam. Hydrol.*, *1*, 407–424.

Lenormand, R., E. Touboul, and C. Zarcone (1988), Numerical-models and experiments on immiscible displacements in porous-media, *J. Fluid. Mech.*, *189*, 165–187.

Manthey, S. (2006), Two-phase flow processes with dynamic effect in porous media- parameter estimation and simulation, PhD Dissertation thesis, 212 pp., University of Stuttgart, Germany.

Manthey, S., S. M. Hassanizadeh, and R. Helmig (2005), Macro-scale dynamic effects in homogeneous and heterogeneous porous media, *Transp. Porous Media*, *58*(1–2), 121–145.

Manthey, S., S. M. Hassanizadeh, R. Helmig, and R. Hilfer (2008), Dimensional analysis of two-phase flow including a rate-dependent capillary pressure-saturation relationship, *Adv. Water Resour.*, *31*(9), 1137–1150.

Mirzaei, M., and D. B. Das (2007), Dynamic effects in capillary pressure-saturations relationships for two-phase flow in 3D porous media: Implications of micro-heterogeneities, *Chem. Eng. Sci.*, *62*(7), 1927–1947.

Munson, B. R., D. F. Young, and T. H. Okiishi (1990), *Fundamentals of Fluid Mechanics*, 6th ed., 860 pp., John Wiley, Hoboken, N. J.

O'Carroll, D. M., T. J. Phelan, and L. M. Abriola (2005), Exploring dynamic effects in capillary pressure in multistep outflow experiments, *Water Resour. Res.*, *41*(11), W11419, doi:10.1029/2005WR004010.

O'Carroll, D. M., K. G. Mumford, L. M. Abriola, and J. I. Gerhard (2010), Influence of wettability variations on dynamic effects in capillary pressure, *Water Resour. Res.*, *46*(8), W08505, doi:10.1029/2009WR008712.

Oung, O., S. M. Hassanizadeh, and A. Bezuijen (2005), Two phase flow experiments in a geocentrifuge and the significance of dynamic capillary pressure, *J. Porous Media*, *8*(3), 247–257.

Rosenbaum, U., J. A. Huisman, A. Weuthen, H. Vereecken, and H. R. Bogena (2010), Sensor-to-sensor variability of the ECH2O EC-5, TE, and 5TE sensors in dielectric liquids, *Vadose Zone J.*, *9*(1), 181–186.

Roth, K., R. Schulin, H. Fluhler, and W. Attinger (1990), Calibration of time domain reflectometry for water-content measurement using a composite dielectric approach, *Water Resour. Res.*, *26*(10), 2267–2273, doi:10.1029/WR026i010p02267.

Sakaki, T., A. Limsuwat, K. M. Smits, and T. H. Illangasekare (2008), Empirical two-point A-mixing model for calibrating the ECH2O EC-5 soil moisture sensor in sands, *Water Resour. Res.*, *44*, W00D08, doi:10.1029/2008WR006870.

Sakaki, T., D. M. O'Carroll, and T. H. Illangasekare (2010), Dynamic effects in field soil water retention curves: Direct laboratory quantification of dynamic coefficient for drainage and wetting cycles, *Vadose Zone J.*, *9*, 424–437.

Selker, J., P. Leclerq, J. Y. Parlange, and T. Steenhuis (1992), Fingered flow in 2 dimensions. 1. Measurement of matric potential, *Water Resour. Res.*, *28*(9), 2513–2521, doi:10.1029/92WR00963.

Silin, D., and T. Patzek (2004), On Barenblatt's model of spontaneous countercurrent imbibition. *Transp. Porous Media*, *54*, 297–322.

Smiles, D. E., G. Vachaud, and M. Vauclin (1971), A test of the uniqueness of the soil moisture characteristic during transient, nonhysteretic flow of water in a rigid soil, *Soil Sci. Soc. Am. J.*, *35*(4), 534–539.

Stauffer, F. (1978), Time Dependence of the Relations between Capillary Pressure, Water Content and Conductivity During Drainage of Porous Media, paper presented at IAHR Symp. on Scale Effects in Porous Media, Thessaloniki, Greece.

Topp, G. C., A. Klute, and D. B. Peters (1967), Comparison of water content-pressure head data obtained by equilibrium, steady-state, and unsteady-state methods, *Soil Sci. Soc. Am. J.*, *31*(3), 312–314.

van Genuchten, M. T. (1980), A closed form equation for predicting the hydraulic conductivity of unsaturated soils, *Soil Sci. Soc. Am. J.*, *44*, 892–898.

Wildenschild, D., J. W. Hopmans, and J. Simunek (2001), Flow rate dependence of soil hydraulic characteristics, *Soil Sci. Soc. Am. J.*, *65*(1), 35–48.

G. Goel, Department of Civil Engineering, School of Engineering and Technology, Sharda University, Plot 32-34, Knowledge Park III, Greater Noida, Uttar Pradesh 201306, India.

D. M. O'Carroll, Department of Civil and Environmental Engineering, University of Western Ontario, London, ON N6A 5B9, Canada. (docarroll@eng.uwo.ca)